Measurement of Pharmacokinetics of Yttrium-86 Radiopharmaceuticals with PET and Radiation Dose Calculation of Analogous Yttrium-90 Radiotherapeutics

Hans Herzog, Frank Rösch, Gerhard Stöcklin, Christoph Lueders, Syed M. Qaim and Ludwig E. Feinendegen

This article and updated information are available at:
http://jnm.snmjournals.org/content/34/12/2222

Information about reproducing figures, tables, or other portions of this article can be found online at:
http://jnm.snmjournals.org/site/misc/permission.xhtml

Information about subscriptions to JNM can be found at:
http://jnm.snmjournals.org/site/subscriptions/online.xhtml

SNMMI | SOCIETY OF NUCLEAR MEDICINE AND MOLECULAR IMAGING

Measurement of Pharmacokinetics of Yttrium-86 Radiopharmaceuticals with PET and Radiation Dose Calculation of Analogous Yttrium-90 Radiotherapeutics

Hans Herzog, Frank Rösch, Gerhard Stöcklin, Christoph Lueders, Syed M. Qaim and Ludwig E. Feinendegen

Institutes of Medicine and Nuclear Chemistry, Research Center Jülich, Jülich, Germany

This study was performed to demonstrate the quantitative in vivo assessment of human pharmacokinetics of ^{90}Y-radiotherapeutics using the positron-emitting substitute ^{86}Y and PET. This technique is illustrated in a patient with disseminated bone metastases from breast cancer who was injected with 100 MBq of ^{86}Y-citrate as an analog of the commercially available radiotherapeutic ^{90}Y-citrate. Whole-body distribution was measured with a PET camera 4, 10, 21, 28 and 45 hr postinjection. Uptake data were determined from reconstructed transverse PET images by regions of interest placed in normal bone tissue, liver and metastases. Images of coronal and sagittal whole-body sections were obtained by reformatting the transverse PET images. The ratio of activity concentration in metastases to that in normal bone ranged from 1.5:1 to 3.5:1. Of the injected tracer, 13.4% was found in the skeleton and 0.43% in the metastasis with the highest ^{86}Y concentration. Radiation doses per 1 MBq of injected ^{90}Y-citrate were calculated from ^{86}Y-citrate data and data from MIRD pamphlets 5 and 11. The doses were 1.01 MGy/MBq for red marrow, 593 μGy/MBq for the liver and ~3.5 MGy/MBq for the most conspicuous metastases. This study demonstrates that the use of PET via ^{86}Y allows an individual in vivo quantification of activity uptake and radiation dose of both normal tissue and tumor in pain treatment with ^{90}Y-labeled radiotherapeutics.

J Nucl Med 1993; 34:2222–2226

This paper presents an in vivo method to assess the pharmacokinetics of ^{90}Y-radiotherapeutics quantitatively using the positron emitter ^{86}Y ($T_{1/2}$ = 14.74 hr, β^+ = 33%, $E_{\beta^+,max}$ = 1.4 MeV) and PET. It focuses on a general methodological approach to obtain biodistribution, biokinetic and dosimetric data for ^{90}Y-labeled compounds in vivo which can also be applied to other therapeutic isotopes.

Of various beta-emitting radioisotopes, such as ^{32}P, ^{89}Sr, ^{131}I, ^{153}Sm or ^{186}Re, used for treatment of painful bone metastases (1–6), ^{90}Y offers some advantages: (1) it is available in a convenient generator system for no-carrier-added synthesis; and (2) many compounds, including complexes, chelates and particles (3,7–10) and monoclonal antibodies (Mabs) (11–18) can be labeled with ^{90}Y. Recently, improved chemistry for the production of this radioisotope was suggested (19,20). In spite of these advantages, two important problems remain unsolved which pertain also to other beta-emitting radiotherapeuticals: the human pharmacokinetics as well as the internal radiation doses of ^{90}Y-labeled radiopharmaceuticals are not known on a quantitative level.

The general attempt to solve this problem is to substitute ^{90}Y by an yttrium radioisotope detectable noninvasively from outside the body. Although ^{88}Y was studied in animals (21,22) and ^{87}Y in humans (23,24), no data about uptake kinetics or radiation doses were reported. Because PET is capable of measuring biodistribution quantitatively, the positron-emitting ^{86}Y is expected to be the yttrium radioisotope of choice (25). Recently, nuclear data relevant to the production of ^{86}Y via the nuclear reactions ^{86}Sr(p,n) and ^{nat}Rb(^{3}He,2n) as well as cyclotron irradiation, radiochemical processing and quality control were published (26,27).

PET imaging with ^{86}Y-citrate was performed on a patient suffering from several bone metastases. The aim of this study was to demonstrate that the application of an ^{86}Y-labeled radiopharmaceutical in conjunction with PET measurements leads to quantitative data on localization and uptake kinetics, thus allowing calculation of radiation doses to individual metastases and normal tissue in radiotherapy with the ^{90}Y analog.

SUBJECT AND METHODS

Patient

The patient investigated was a 37-yr-old female in whom a malignant tumor of the right breast had been diagnosed 1.5 yr ago. In spite of surgical, radiation and chemotherapies, numerous bone metastases were found 10 mo later and further radiation therapy of the painful bone lesions was carried out several times. Plain x-ray film, computed tomography and bone scintigraphy with

^{99m}Tc-DPD (^{99m}Tc-3,3-diphospono-1,2 propanedicarbonate) recorded before the PET examination revealed metastases in the facial part of the head, the lung, the pelvis, the right femur and at different locations in the spine. A palliative treatment with ^{90}Y-citrate was performed directly after the PET investigation.

Preparation and Application of ^{86}Y-Citrate

Yttrium-86 was produced at the Jülich compact cyclotron CV28 via the (p,n)-reaction on 96.3% enriched ^{86}SrCO$_3$ target material in the proton energy range of 14.2 → 10.2 MeV (26,27). Chemical processing led to no carrier-added and radiochemically pure ^{86}Y(III). Yttrium-86-citrate was synthesized by adding one drop of aqueous ^{86}Y(III) solution to 2 ml of sodium citrate solution (7.5 mg/ml, final pH 7.4). The pharmaceutical was sterile filtered and apyrogenity was ensured by standard methods. Radiochemical quality control was performed by paper chromatography on MN21 using pyridine-to-ethanol-to-water mixtures (4:2:1) as solvent. The content of the ^{86}Y-citrate complex was found to be >98%. Twelve hours after isotope production, 100 MBq of ^{86}Y-citrate were injected intravenously. As detected by gamma-ray spectrometry, the radionuclide contaminants of ^{86}Y, namely ^{87m}Y, ^{87}Y and ^{88}Y amounted to 1.9%, 0.75% and 0.1%, respectively, at the time of application.

Measurement and Data Analysis

Four hours after the injection of the radiotracer, the first PET measurement was performed with a whole-body PET camera PC4096-15WB (Scanditronix-GE, Uppsala, Sweden). This camera's field of view has a diameter of 55 cm and a thickness of 10.5 cm in which 15 adjacent planes are recorded simultaneously. Performance characteristics have been described earlier by Rota Kops et al. (28). In order to correct the acquired emission data for attenuation, a sequence of transmission scans was obtained before the first emission scan. This sequence consisted of fourteen 3-min transmission scans between which the patient's bed was moved 10.5 cm in the cranial direction so that the patient was viewed from the head down to the most caudally located metastasis, with a length of 147 cm. Sequences of 4-min emission scans with identical movements of the patient's bed were acquired at 4, 10, 21, 28 and 45 hr after tracer injection (p.i.). The patient was very carefully repositioned in order to match the position during the transmission scan.

The reconstruction of the emission data corrected for attenuation resulted in 210 PET images of transverse orientation for each measurement. The tracer accumulation in five prominent metastases and normal bone was quantified by the region of interest (ROI) technique. ROIs over the metastases were manually defined by comparing tracer uptake with their localizations seen in radiological images and bone scintigrams. The activity concentration at a specific uptake site was evaluated in three adjacent slices, averaged and corrected for radioactive decay. Because PET measures only the positron emissions, which are 33% of all radioactive events of ^{86}Y, the activity concentrations found by PET were multiplied by 3.0.

In order to display PET whole-body views of the distribution of ^{86}Y-citrate, a computer program was written, by which the transversal PET images were rearranged as described in the following: Each sequence of 14 × 15 PET images with a matrix size of 256 × 256 were assembled in a three-dimensional matrix containing 210 × 256 × 256 elements. The dimensions of each voxel were 6.5 mm in the axial (z) direction and 2 mm in the x/y-direction. In order to reduce the amount of storage needed, every 2 × 2 pixels in the image plane were combined by averaging. The resulting three-dimensional matrix with its 210 × 128 × 128 elements was filtered with a three-dimensional filter kernel. After reading this file by a second program, any coronal or sagittal section with an area of 147 cm × 51.2 cm could be obtained. In order to achieve the same scale in the z-direction as in the x-direction or the y-direction, data in the z-direction were interpolated.

The calculation of the radiation doses to the red marrow, the liver and the five metastases were performed along the lines suggested by the MIRD Committee (29). The decay-corrected pharmacokinetic data, i.e., percentage of injected ^{86}Y activity per organ or per cm^3 tissue, were considered to also be valid for the ^{90}Y-labeled therapeutic. By extrapolating this data until five half-times of ^{90}Y (T_5), multiplying them with the decay function and integrating until T_5, the cumulated activities A were obtained. To get the percentage of injected activity in normal bone and liver, the activity concentration primarily measured by PET was multiplied by the organ's volume as given by the MIRD Committee for a human weighing 70 kg (30). Taking into account the patient's weight of 75 kg, a bone tissue density of 1.5 g/cm^3 and a liver density of 1 g/cm^3, the resulting volume of the total bone was about 3600 cm^3 and that of the liver was 1900 cm^3.

The radiation dose to the liver was

$$D_{Liver} = A_{Liver}S_{Liver \to Liver}.$$

The radiation dose to the red marrow (RM), considered to be caused by activity equally stored in cortical and trabicular bone, was obtained by:

$$D_{RM} = A_{Bone}(0.5S_{Cort.Bone \to RM} + 0.5S_{Trab.Bone \to RM}).$$

The S-factors were taken from MIRD Pamphlet no. 11 (29) for ^{90}Y.

The radiation dose to a metastasis D_{Meta} with volume V and mass M = Vρ was calculated by:

$$D_{Meta} = \frac{A_{Meta}V\phi\Delta}{M} = \frac{A_{Meta}\phi\Delta}{\rho},$$

with A_{Meta} = cumulated activity per injected 1 MBq per 1 cm^3 of metastatic tissue; $\phi\Delta$ = absorbed dose fraction times dose constant for ^{90}Y = 2 g rad/(μCi hr) = 0.54 g Gy/(MBq hr); and ρ = bone density = 1.5 g/cm^3.

Therefore, the dose to a metastasis is dependent only on the activity concentration as measured by PET and not on its volume.

RESULTS

Figure 1 (left part) displays an anterior view of the patient's body from the head down to the knee. As all coronal sections are summarized here, this image is equivalent to the conventional whole-body scan obtained with a gamma camera. However, the data here are corrected for attenuation. The locations of increased tracer uptake are in agreement with the hot spots found in the bone scintigrams with ^{99m}Tc-DPD (Fig. 2). As expected, a general bone uptake of ^{86}Y was found. Furthermore, ^{86}Y was observed also in the liver. The right part of Figure 1 represents a sagittal 8 cm thick section in the median plane of the patient's body. Here the metastases in the spine are clearly displayed.
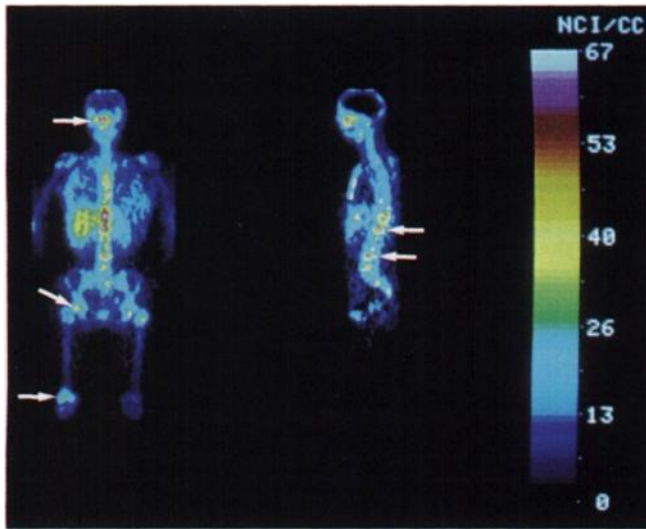
FIGURE 1. Whole-body images of the distribution of ^{86}Y-citrate in a 37-yr-old female at 10 hr postinjection. Left: anterior view with all coronal sections summed up. Right: 8-cm thick sagittal section in the median plane of the patient's body. The arrows indicate the five metastases which were evaluated.

FIGURE 2. Bone scintigrams after injection of ^{99m}Tc-DPD shows bone metastases in the head, spine, pelvis and knee.

FIGURE 3. Decay-corrected time-activity curves of ^{86}Y-citrate in normal bone (spine), liver and five metastases.

Table 1 summarizes the quantitative, decay-corrected data of ^{86}Y uptake in normal spine, liver and five different metastases. The coefficient of variance (i.e., s.d. related to the mean) of the pixel activities in the single ROIs ranged from 30% to 100%. The uptake kinetics of ^{86}Y-citrate are shown in Figure 3.

The activity concentration in the normal spine was practically constant with about 4 kBq/cm^3 from 10 hr postinjection until the last measurement at 45 hr postinjection. Using this activity concentration as representative for normal bone, 13.4% of the injected yttrium was stored in the skeleton. As the same uptake data would have been ob-
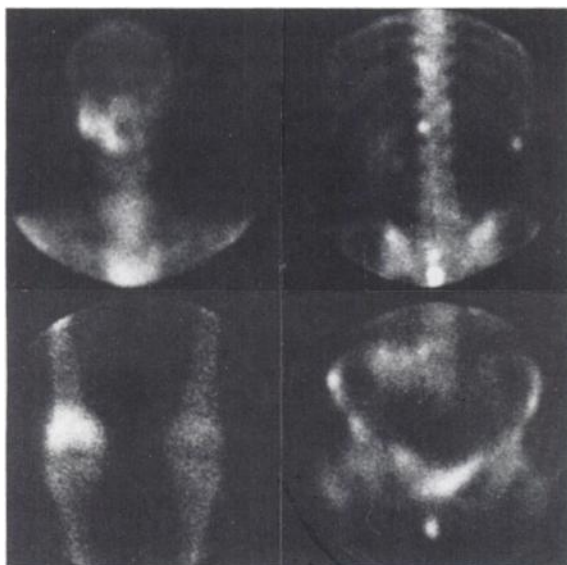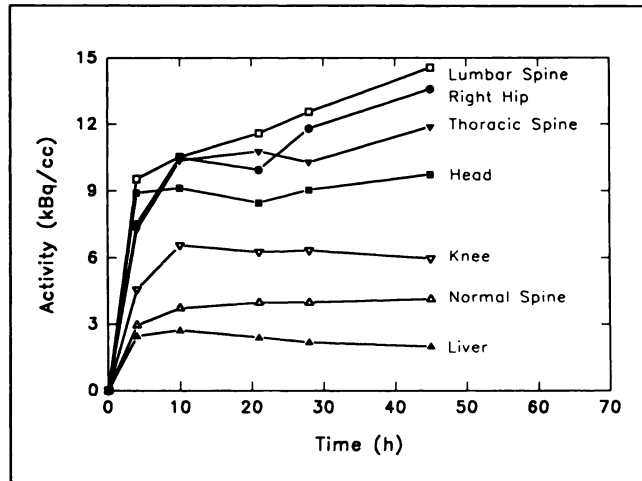
tained if ^{90}Y-citrate instead of ^{86}Y-citrate had been injected, these data yield a radiation dose to the nonaltered red marrow of 1008 μGy per 1 MBq of injected ^{90}Y-citrate.

In the anterior whole-body image (Fig. 1, left) the liver is clearly visible. In contrast to the bone uptake, the liver activity decreased steadily from 10 hr to 45 hr postinjection. With an activity concentration of 2.56 kBq/cm^3 and an estimated liver volume of 1900 cm^3 (see above), 4.5% of the injected dose was found in the liver at 4 hr postinjection. These data resulted in a radiation dose of 593 μGy per 1 MBq of injected ^{90}Y-citrate.

The uptake of ^{86}Y in the head metastases, the thoracic spine, and the right knee was nearly constant after 10 hr postinjection. The metastases in the hip and the lumbar spine seem to accumulate ^{86}Y until 45 hr postinjection, however, the activity concentrations measured at 45 hr postinjection are not statistically sound since they were very low with a coefficient of variance of up to 100%. Furthermore, the error might have been enhanced by the decay correction. Therefore, the calculation of radiation dose in bone and metastases assumed a constant activity concentration after 10 hr postinjection. The activity concentration found in the metastases is higher than in normal bone (spine) with a ratio between 1.5 and 3.5:1 (Table 2). The maximum activity concentration was observed in the metastasis located in the lumbar spine with about 0.43% of the injected dose at 10 hr postinjection. For this calculation, the volume of the metastasis was determined to be about 40 cm^3 by ROI measurements. The radiation dose to the five evaluated metastases ranged from 2.1 to 3.5 mGy per 1 MBq of ^{90}Y-citrate (Table 3).

DISCUSSION

In this study, 100 MBq of ^{86}Y-citrate were injected in a patient suffering from multiple bone metastases from breast cancer. In spite of the low activity of the injected tracer and a low abundance of 33% positron decays of ^{86}Y,

TABLE 1
Activity Concentration (kBq/cc) of Yttrium-86 in Normal Bone, Liver and Five Different Metastases

Time of scan (hr)	Normal spine	Liver	Metastases				
			Head	Thoracic spine	Lumbar spine	Hip	Knee
4	2.94	2.46	8.91	7.26	9.54	7.50	4.56
10	3.72	2.73	9.15	10.38	10.53	10.50	6.57
21	3.96	2.40	8.49	10.80	11.61	9.96	6.27
28	3.96	2.19	9.09	10.32	12.60	11.79	6.36
45	4.11	2.01	9.78	11.94	14.64	13.59	5.91

the PET measurements yielded quantitative data on tracer uptake in normal bone and metastases.

The short recording time of 4 min for each 10.5-cm section of the patient's body and the low number of coincidence events with a maximum of about 25,000 at 4 hr postinjection and 3,300 at 45 hr postinjection for a single plane resulted in a high noise level of the single reconstructed PET images. When these PET images were assembled into a large set of three-dimensionally filtered volume data, cross-sectional whole-body images with a very good quality could be obtained. Similar images have recently been published by Dahlbom et al. (31). In their study, ^{18}F-fluorodeoxyglucose and the ^{18}F ion were used as tracers and the quality of the whole-body images was excellent. However, those authors injected 370 MBq of the tracer with 100% positron decays. Taking into account these differences, the quality of the whole-body images of [86]Y is surprisingly good.

As expected, [86]Y-citrate was primarily taken up by bone. The accumulation in the various bone metastases was higher than in the normal bone with factors ranging between 1.5 and 3.5:1 so that the metastases could clearly be delineated. The results found for the liver in comparison to those for the skeleton are understandable in terms of different uptake retention mechanisms of [86]Y-citrate in the two organs concerned. Considering recent pharmacokinetic data on [153]Sm-EDTMP in rats and humans (32–34) and first results of the biodistribution of [88]Y-EDTMP in rats (21), which both recorded a missing liver accumulation, one could avoid the [86]Y-activity uptake in the liver by replacing citrate with EDTMP.

Based on the quantitative data of uptake kinetics of [86]Y-citrate, radiation doses were calculated which would

be caused by ^{90}Y-citrate. Because of the shorter half-life of [86]Y (14.7 hr) compared to that of [90]Y (64 hr), the assumption of a constant storage of yttrium in the metastasis and the skeleton is critical. This assumption is, however, supported by the results of Kutzner et al. (22). In our own data we found a nearly constant activity concentration (corrected for decay) in the normal bone and in the metastases in the head, the thoracic spine and the right knee. In the other metastases, the results for the last measurement at 45 hr postinjection differed from a plateau-like uptake. These results, however, might be erroneous, because the ROI data revealed a very high noise level. Therefore, the increases in [86]Y-activity do not disprove the assumption of constant storage of yttrium in normal and tumor-containing bones.

In contrast to conventional approaches, where only a total bone uptake of a radiotherapeutic is determined by the difference of injected and urinarily excreted activity, the method reported here is able to yield individual dose estimates to the red marrow and to single metastases. The calculations of the radiation dose per 1 MBq of ^{90}Y-citrate injected, yielded 593 μGy for the liver, 1008 μGy for the red marrow and about 3.5 mGy to the metastases with the highest uptake. The radiation dose to these metastases was more than three times higher than the dose to the red marrow. The calculation of the radiation dose is based on ROI evaluation which yields average data for a metastasis in total. It is, however, expected that the radiation dose is higher in those parts of a metastasis which show peaks of tracer accumulation.

The findings presented in this paper for the first patient have to be verified in a greater number of cases and completed with further data for blood clearance and urinary excretion. Furthermore, it would be interesting to compare "[86]Y/PET-evaluated" ^{90}Y-citrate with other ^{90}Y com-

TABLE 2
Activity Concentration of Yttrium-86 in Five Metastases Normalized to Activity Concentration in Normal Spine

Time of scan (hr)	Head	Thoracic spine	Lumbar spine	Hip	Knee
4	3.0	2.5	3.2	2.5	1.5
10	2.6	2.8	2.8	2.8	1.8
21	2.1	2.7	2.9	2.5	1.6
28	2.3	2.6	3.2	2.5	1.6
45	2.4	2.9	3.6	3.3	1.4

TABLE 3
Radiation Dose (mGy/MBq) of Yttrium-90 to Red Marrow, Liver and Five Different Metastases

Red marrow	Liver	Metastases				
		Head	Thoracic spine	Lumbar spine	Hip	Knee
1.01	0.59	2.94	3.34	3.47	3.37	2.12

pounds like ^{90}Y-EDTMP and these with recently considered radiotherapeuticals like ^{153}Sm-EDTMP (5,32–34) or ^{186}Re-HEDP (6). For the latter compounds, tumor-to-bone ratios have been found with animal research and/or conventional whole-body scintigraphy or SPECT, which are similar to or better than the ratios found here for ^{90}Y-citrate.

Rather than to compare different radiotherapeuticals relevant for bone pain treatment, the purpose of this paper was to describe the methodology. Our example demonstrates that quantification of human pharmacokinetics and radiation doses of the therapeutically used beta-emitting isotope ^{90}Y is possible with PET measurements using its beta-emitting sister isotope ^{86}Y.

REFERENCES

1. Kaplan E, Fels IG, Kotlowski BR, et al. Therapy of carcinoma of the prostate metastatic to bone with ^{32}P-labeled condensed phosphate. *J Nucl Med* 1960;1:1–13.
2. Firusian N, Mellin P, Schmitt CG. Results of strontium-89 therapy in patients with carcinoma of the prostate and incurable pain from bone metastases: a preliminary report. *Urol* 1976;116:764–768.
3. Kutzner J, Dähnert W, Schreyer T, Grimm W, Brod KH, Becker M. Yttrium-90 zur Schmerztherapie von Knochenmetastasen. *Nucl Med* 1981; 20:229–235.
4. Eisenhut M, Berberich R, Kimmig B, Oberhausen E. Iodine-131-labeled diphosphonates for palliative treatment of bone metastases: II. Preliminary clinical results with iodine-131 BDP 3. *J Nucl Med* 1986;27:1255–1261.
5. Goeckeler WF, Edwards B, Volkert WA, Holmes RA, Simon J, Wilson D. Skeletal localization of samarium-153 chelates: potential therapeutic bone agents. *J Nucl Med* 1987;28:495–504.
6. Ketring A. ^{153}Sm-EHDP and ^{186}Re-HEDP as bone therapeutic radiopharmaceuticals. *Nucl Med Biol* 1987;14:223–232.
7. Dunscombe PB, Ramsey NW. Radioactivity studies on two synovectomy specimens after radiation synovectomy with yttrium-90 silicate. *Ann Rheum Dis* 1985;39:87–89.
8. Bowen BM, Darracott J, Garnett ES, Tomlinson RH. Yttrium-90 citrate colloid for radioisotope synovectomy. *A J Hosp Pharm* 1975;32:1027–1030.
9. Greiff R. Zur durchführung der schmerztherapie von knochenmetastasen mit ^{90}Y-zitrat. *Nucl Med* 1989;1:93–96.
10. Shapiro B, Andrews J, Figg L, et al. Therapeutic intraarterial administration of yttrium-90 glass microspheres for hepatic tumours [Abstract]. *Eur J Nucl Med* 1989;8:401.
11. Hantovitch DJ, Virzi F, Doherty PW. DTPA-coupled antibodies labeled with yttrium-90. *J Nucl Med* 1985;26:503–509.
12. Vaughan ATM, Keeling A, Yankuba SCS. The production and biological distribution of yttrium-90-labeled antibodies. *Int J Appl Radiat Isot* 1985; 36:803–806.
13. Washburn LC, Sun TT Hwa, Crook JE, et al. Yttrium-90-labeled monoclonal antibodies for cancer therapy. *Nucl Med Biol* 1986;13:453.
14. Order SE, Klein JL, Leichner PL, Frinke J, Lollo C, Carlo DJ. Yttrium-antiferritin—a new therapeutic radiolabeled antibody. *Int J Radiat Oncol Biol Phys* 1986;12:277–281.
15. Anderson-Berg WT, Squire RA, Strand M. Specific radio-immunotherapy using ^{90}Y-labeled monoclonal antibody in erythroleukemic mice. *Cancer Res* 1987;47:1905–1912.
16. Leichner PK, Yang NC, Frenkel TL, et al. Dosimetry and treatment planning for ^{90}Y-labeled antiferritin in hepatoma. *Int J Radiat Oncol Biol Phys* 1988;14:1033–1042.
17. Kozak RW, Raubitschek A, Mirzadeh S, et al. Nature of the bifunctional chelating agent used for radioimmunotherapy with yttrium-90 monoclonal antibodies: critical factors in determining in vivo survival and organ toxicity. *Cancer Res* 1989;49:2639–2644.
18. Hird V, Stewart JSW, Snook D, et al. Intraperitoneally administered ^{90}Y-labeled monoclonal antibodies as a third line of treatment of ovarian cancer. A phase 1-2 trial: problems encountered and possible solutions. *Br J Cancer* 1990;62(suppl 10):48–51.
19. Dietz ML, Horwitz EP. Improved chemistry for the production of yttrium-90 for medical applications. *Int J Appl Radiat Isot* 1992;43:1093–1101.
20. Bray LA, Wheelwright EJ, Wester DW, et al. Production of ^{90}Y at Hanford [Abstract]. *J Nucl Med* 1991;32:1090.
21. Beyer GJ, Bergmann R, Kampf G, Mäding P, Rösch F. Simultaneous study of the biodistribution of radio-yttrium complexed with EDTMP and citrate ligands in tumour-bearing mice. *Nucl Med Biol* 1992;19:201–203.
22. Kutzner J, Mittas W, Grimm W. Verteilungsmuster bei ratten nach intravenöser injektion von ^{88}Y-verbindungen. *Nucl Med* 1981;20:35–39.
23. Buchali K, Haesner M, Lips H, Beyer GJ, Rösch F, Pink V. Strontium-89 versus ^{90}Y-citrate for palliation of skeletal metastases. Preliminary results of a controlled study [Abstract]. *Eur J Nucl Med* 1991;18:529.
24. Kutzner J, Hahn K, Beyer GJ, Grimm W, Bockisch A, Rösler HP. Szintigraphische verwendung von ^{87}Y bei der ^{90}Y-therapie von knochenmetastasen. *Nucl Med* 1992;31:53–56.
25. Rösch F, Beyer GJ. Längerlebige positronen-emitter: einzelnuklide und generatorsysteme, herstellung am U-120-zyklotron in Rossendorf, radiochemische studien sowie möglichkeiten für die PET. *Report ZfK-745* 1991;1–30.
26. Rösch F, Qaim SM, Stöcklin G. Nuclear data relevant to the production of the positron emitting radioisotope ^{86}Y via the ^{86}Sr(p,n)- and natRb(3He,2n)-processes. *Radiochim Acta* 1993;61:1–8.
27. Rösch F, Qaim SM, Stöcklin G. Production of the positron emitting radioisotope ^{86}Y for nuclear medical application. *Int J Appl Radiat Isot* 1993;44: 677–681.
28. Rota Kops E, Herzog H, Schmid A, Holte S, Feinendegen LE. Performance characteristics of an eight-ring whole-body PET scanner. *J Assist Comput Tomogr* 1990;14:437–445.
29. Snyder WS, Ford MR, Warner GG, Watson SB. "S," absorbed dose per unit cumulated activity for selected radionuclides and organs. *MIRD pamphlet no. 11.* New York: Society of Nuclear Medicine, 1975.
30. Snyder WS, Ford MR, Warner GG, Fisher HL, Jr. Estimates of absorbed fractions for monoenergetic photon sources uniformly distributed in various organs of a heterogeneous phantom. *MIRD pamphlet no. 5.* *J Nucl Med* 1969;10(suppl. 3):5–52.
31. Dahlbom M, Hoffman EJ, Hoh CK, et al. Whole-body positron emission tomography: part I. Methods and performance characteristics. *J Nucl Med* 1992;33:1191–1199.
32. Turner JH, Martingale AA, Sorby P, et al. Samarium-153-EDTMP therapy of disseminated skeletal metastasis. *Eur J Nucl Med* 1989;15:784–795.
33. Singh A, Holmes RA, Farhangi M, et al. Human pharmacokinetics of samarium-153-EDTMP in metastatic cancer. *J Nucl Med* 1989;30:1814–1819.
34. Eary J, Collins C, Stabin M, et al. Samarium-153-EDTMP biodistribution and dosimetry estimation. *J Nucl Med* 1993;34:1031–1036.